Sizing of Hybrid Energy Storage System for Residential PV Applications

Xiangqiang Wu, Zhongting Tang, Tamas Kerekes
Aalborg University
Pontoppidanstræde 101, 9220 Aalborg East
Aalborg, Denmark
Tel.: +45 91868836
Fax: +45 99408540
E-Mail: xiwu@energy.aau.dk
URL: https://www.en.aau.dk/

Keywords

« Photovoltaic», « Energy storage», « Battery », « Supercapacitor».

Abstract

In this paper, a sizing methodology is proposed for a grid-connected PV and hybrid energy storage system, which is used to determine the capacity share ratio of the Li-ion battery and the supercapacitor. Based on one case of the PV and the load mission profiles, the proposed sizing scheme can reduce the cycle numbers of the Li-ion battery and utilize the supercapacitor most, hence improving the self-consumption of the PV system with hybrid energy storage.

Introduction

Photovoltaic (PV) energy has grown rapidly in the last few decades due to global environmental awareness. However, managing PV production is challenging due to its intermittency and un-prediction, which means a huge amount of fluctuating power will be injected into the distribution systems. Therefore, solutions to flexibly control become mandatory tasks for PV systems [1].

In order to provide a reliable operation of PV systems, batteries are seen as a promising solution due to their decreasing prices, easy scalability, and flexibility. In addition, with the decreasing feed-in tariffs and increasing prices of grid electricity, maximum self-consumption operation of the PV generated electricity is becoming more attractive than feeding energy into the grid. In this case, optimal sizing of the energy storage system in grid-connected PV systems is a crucial issue, which relates to the reliable and economical system operation, and contributes to the more widespread use of batteries in PV applications. In this regard, much literature has proposed various sizing methods based on different evaluation objectives, which can be briefly categorized into three types: levelized cost of energy (LCOE) [2]-[4], power autonomy [5], and battery lifetime [6]-[8].

In addition, due to the changing solar irradiance and ambient temperature, there exist fluctuating PV power, which may decrease the lifespan of batteries and challenge the stable operation of the grid. Thus, that should be paid more attention to the dynamic response and battery lifetime. In recent years, hybrid energy storage systems (HESS) have drawn more attention since they can provide more control flexibility than that with battery only. Besides, HESS can extend the lifetime of batteries to some extent, which may make it a more cost-effective solution in energy storage applications [9]-[11]. Nevertheless, the optimal sizing criteria are not clear in prior-art literature, leading to the oversize of some storage elements and poor cost-effectiveness of the system.

This paper focuses on the optimal sizing of the hybrid energy storage system (i.e., Li-ion battery and supercapacitor) for residential PV applications. Based on given PV and load profiles, a sizing scheme is proposed to maximize the utilization of the supercapacitor and improve the self-consumption of the PV system. Firstly, the PV system configuration is presented, and a set of full-year PV and load profiles are adopted in this case. Secondly, the cycles of the battery and supercapacitor are presented and discussed

considering the influences of the time constant of the low-pass filter. Then, the optimal sizing method is proposed based on the utilization of the supercapacitor and self-consumption of the system. The conclusion is presented in the last section.

System Configuration

Schematic

Fig. 1 shows the integrated PV and energy storage system, which consists of PV arrays, a hybrid energy storage system (i.e., Li-ion battery and supercapacitor), load, and the grid. In Fig. 1, the black arrows represent electrical links, while blue dashed arrows represent power flow directions. The battery and supercapacitor are parallel to each other in an active connection [12], which provides more control degrees of freedom. In this system, PV, battery, and supercapacitor connect the same DC bus through separate DC-DC converters, and P_{PV}, P_{bat}, P_{SC} are respectively output power of PV, battery, and supercapacitor. ΔP_{grid} is the power difference between PV production and energy storage, and P_{grid} is the power injected or absorbed from the grid.

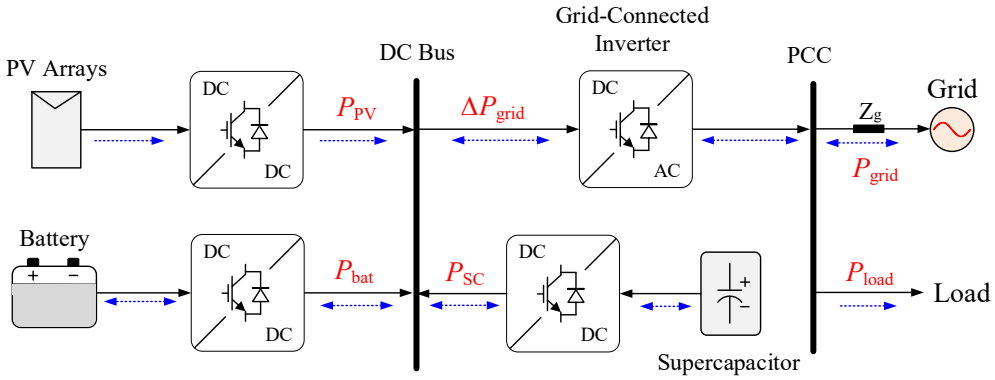

Fig. 1: Structure of the PV-HESS system.

Input Data

To analyze the power flows in the PV-HESS system of a typical household, a simulation model is developed. Both PV profile and load data sets are used as input for the simulation, which are shown in Fig. 2. In Fig. 2(a), the ambient temperature and solar irradiance are represented by a blue curve and orange curve, respectively, and these data are recorded for a full year with one-minute resolution in Aalborg, Denmark, located at 57° N, 9° E. The load profile of a typical Danish household is shown in Fig. 2(b), whose annual electricity consumption is about 3 MWh.

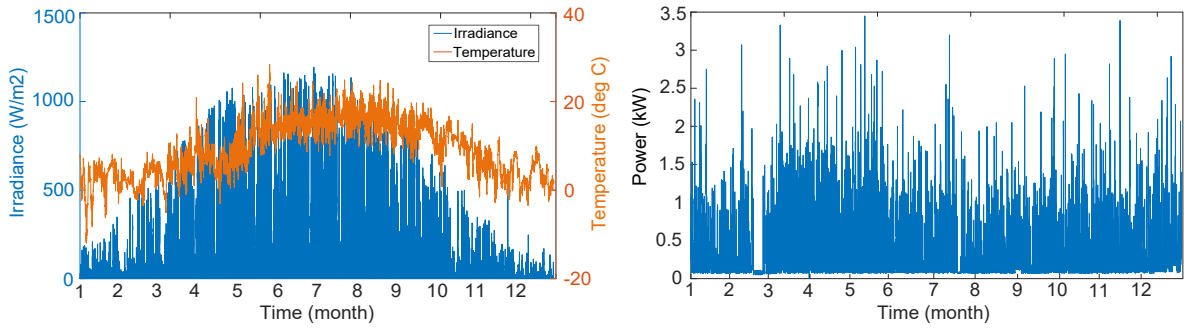

(a) (b)

Fig. 2: PV and load profiles: (a) PV data; (b) load data.

In this paper, the PV model is based on the power temperature coefficient model [13], which is used solar irradiance and ambient temperature to estimate the generated power from the PV panels. The PV power P_{mp} at the maximum power point can be expressed as:

$$P_{\mathrm{mp}}\left(G_{\mathrm{e}},T_{\mathrm{c}}\right)=\frac{G_{\mathrm{e}}}{G_{\mathrm{STC}}}P_{\mathrm{mp,STC}}\left[1+\gamma_{\mathrm{mp}}\left(T_{\mathrm{c}}-T_{\mathrm{STC}}\right)\right] \tag{1}$$

where G_{e} is the effective solar irradiance and G_{STC} is the solar irradiance under standard test condition (STC). $P_{\mathrm{mp,STC}}$ and γ_{mp} are the measured peak power under STC and the normalized temperature coefficient of peak power, respectively. T_{c} and T_{STC} are the solar cell temperature and the temperature at STC conditions.

In this paper, the temperature coefficient is set to -0.35%/°C, and PV generator losses are considered as 8%. The efficiency of power electronic devices in this system is set to 95% at their nominal power. In addition, considering the power distribution between different power sources, the throughput model [14] is adopted to represent the Li-ion battery and supercapacitor, where the number of storage cycles n_{c} can be calculated as follows:

$$n_{c}=\frac{E_{\mathrm{c}}+E_{\mathrm{d}}}{2E_{\mathrm{s}}} \tag{2}$$

where E_{c} and E_{d} are the energy charged and discharged to the battery/SC, respectively. E_{s} is the capacity of the battery/SC.

Based on the input data and simulation model described above, the PV and battery capacity can be sized. Here, the economic evaluation is performed based on the degree of self-sufficiency (d), which is used to qualify the energy independence (i.e., energy autonomy) of the microgrid from the utility grid. It represents the ratio of the load consumption (E_{l}) supplied by the PV-HESS system (including the directly used energy E_{du} and energy discharged for the load E_{d}), which can be expressed as:

$$d=\frac{E_{\mathrm{du}}+E_{\mathrm{d}}}{E_{\mathrm{l}}}\times 100\% \tag{3}$$

Limited by the total investment, the PV and battery capacities are restricted to 10 kWp and 10 kWh respectively. In Fig. 3, the relationship among the self-sufficiency (i.e., power autonomy) of the system, PV, and battery capacity is presented. It can be observed that the ramp rate of self-sufficiency becomes much smaller when it is over 75%, which means a lot of extra investment can gain only a little power autonomy improvement. Therefore, it is reasonable to set the self-sufficiency to 75% by trading off the cost and self-sufficiency rate. In this case, the PV capacity is set to 10 kWp and the battery capacity is set to around 6 kWh.

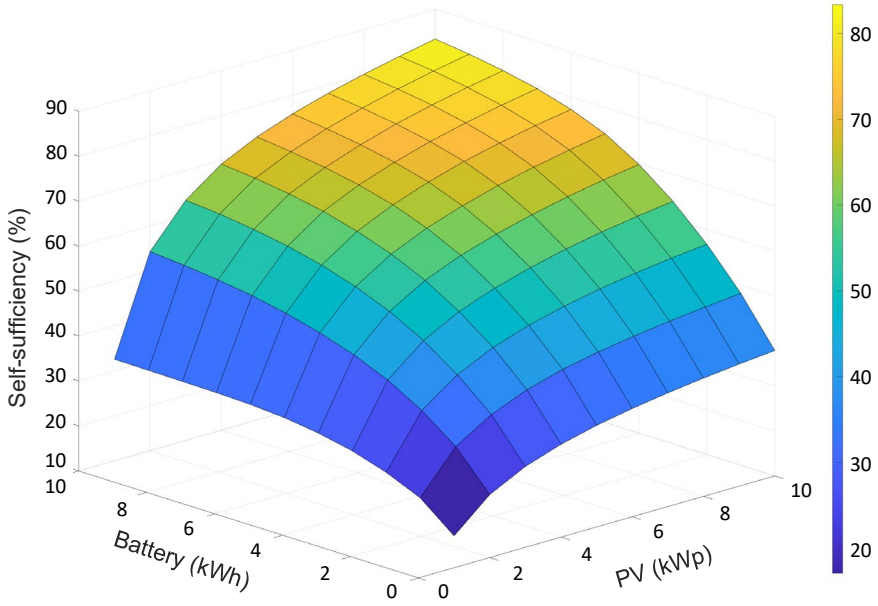

Fig. 3: Trend of self-sufficiency according to the PV and battery capacity

Control Strategy

In this paper, the DC link voltage is controlled by the inverter, and HESS is responsible to maintain the power level injected into the grid. The control framework of power distribution scheme is shown in Fig. 4, where the difference between PV production P_{pv_r} and load power P_{load_r} serves as the reference power of HESS. Through a first-order low-pass filter (LPF) and ramp rate limiter, the reference power of battery P_{bat_r} can be obtained, and the reference power of supercapacitor P_{SC_r} can be obtained by subtracting P_{bat_r} from the reference power of HESS P_{HESS_r}.

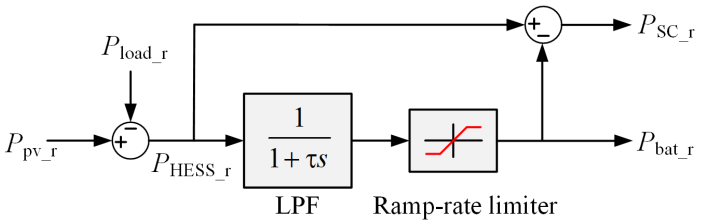

Fig. 4: Power distribution scheme

LPF-based power distribution strategy has been widely used due to its simplicity and superior performance. By changing the LPF time constant τ, the frequency of the current flowing through the battery can be changed. As a consequence, the low-frequency components in the input power will serve as the reference power for the battery, and the high-frequency components become the reference power for the supercapacitor, which accords with the characteristics of different energy storage elements. Considering that high-frequency components are harmful to batteries, the battery lifetime and efficiency of batteries can be improved by adopting supercapacitors with good dynamics. Therefore, an appropriate time constant of LPF and proper supercapacitor capacity are essential for the optimal HESS operation.

Simulation Results and Discussion

In order to size the supercapacitor in the HESS, the relationship among battery and supercapacitor cycles and control parameters (time constant of LPF) should be investigated. Due to the fact that supercapacitors have a much longer lifetime (e.g., over 500000 cycles) than batteries, the optimal supercapacitor size should be where the supercapacitor can gain the most cycles so that the supercapacitor can be utilized to the greatest extent.

Based on the above data and analysis, the simulation model was developed in MATLAB 2021b. The battery capacity is 6144 Wh in the simulation, consisting of twelve 12.8 V/40 Ah Li-ion battery cells. Considering that the battery response time (i.e., the time for a battery to provide energy at its full rated power) is 30 seconds or more, we mainly focus on the time constant over 30 seconds. In the simulation, a series of time constants are studied, which are 1, 30, 60, 120, 360, 600, 1200, 3600, and 6000 seconds. And the state of charge (SOC) of the battery and supercapacitor are both restricted to a range between 10% and 90% of their nominal capacities.

The relationship among supercapacitor cycles, capacities, and time constants is shown in Fig. 5(a). It can be seen that when the capacity of the supercapacitor is fixed, the cycles will increase at first and decrease later with an increasing time constant of LPF. For example, in the case of a 64 Wh supercapacitor, the supercapacitor cycles will increase from 2431 (τ =30 s) to 4236 (τ =360 s), then decrease to 2111 (τ =6000 s). This is because when the time constant increases, the power reference for the supercapacitor will increase as well. However, once the time constant reaches a certain value, the supercapacitor will be fully charged or discharged quickly, so that more energy will flow into the grid instead of the supercapacitor. In Fig.5(a), we can also observe that the time constant for peak supercapacitor cycles will change according to different supercapacitor capacities, and the bigger the supercapacitor size, the larger time constant is needed for peak cycles. Specifically, when the supercapacitor size is between 64 Wh to 128 Wh, the time constant is 360s for peak cycles, while 600s is for the supercapacitor ranging from 128 Wh to 448 Wh. And when the supercapacitor is larger than 448 Wh, a 1200s or higher time constant is needed.

Fig.5(b) shows the total energy injected into and absorbed from the grid. With an increasing time constant of the low-pass filter, the energy flowing through the inverter is increasing as well, which illustrates that there is more energy exchanged between the PV system and the grid. Considering the different prices of feed-in energy and procurement of electricity from the grid, the increasing energy throughput will lower the cost-effectiveness of the system. On the other hand, under a certain time constant, higher supercapacitor capacity leads to lower energy throughput, which means that more energy is consumed on-site, hence the self-consumption will be improved.

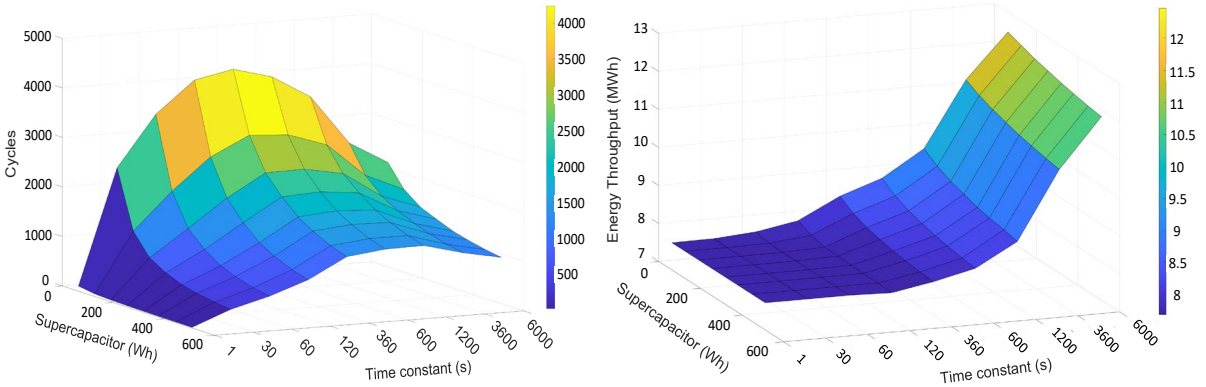

(a) (b)

Fig. 5: Simulation results under different capacities and time constants: (a) supercapacitor cycles; (b) energy throughput to/from the grid.

Based on the above analysis, in order to achieve the best balance between the utilization of the supercapacitor and self-consumption of the system, the time constant is designed to 360 s, and the supercapacitor can be set to 128 Wh (i.e., 1/48 of Li-ion battery). Fig. 6(a) shows the cycles of the Li-ion battery and the energy to/from the grid under different time constants. With a time constant of 360 s, the battery cycles can be reduced by 1.89% compared to that of 1 s time constant. Considering that the high-frequency power fluctuations are filtered, the Li-ion battery lifetime can be prolonged more significantly.

In this case, Fig. 6(b) shows a one-day simulation, where the red curve represents the reference power for the HESS, while the blue and green curves represent the reference power for the battery and the supercapacitor, respectively. The result demonstrates that the high-frequency power fluctuations are charged and discharged through the supercapacitor while the battery mainly deals with the low-frequency power fluctuations. In that case, the battery can obtain some relief effects from the high-frequency harmonics, which can extend the battery lifetime.

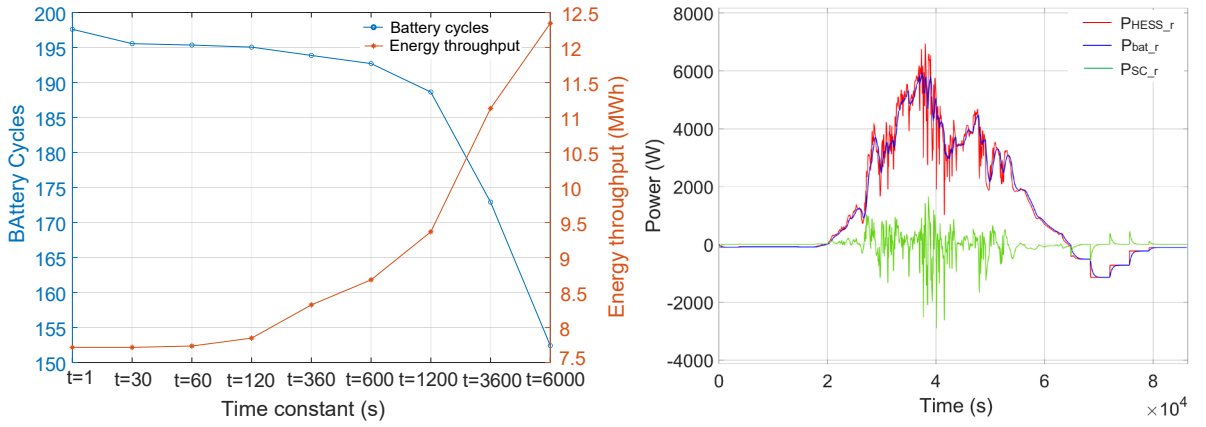

(a) (b)

Fig. 6: Power distribution of the HESS and battery cycles under different time constants: (a) battery cycles and energy throughput; (b) power distribution.

Conclusion

In this paper, the sizing optimization of a grid-connected PV-HESS system is presented. An analysis of LCOE of the PV and the battery is made to size the PV and Li-ion battery capacities firstly. Then, according to the relationship between supercapacitor cycles and the time constant of the LPF, the optimum scaling of the supercapacitor can be determined to achieve maximum utilization of the supercapacitor. Meanwhile, the self-consumption of the PV system can be improved. The results obtained from the simulation show that the sizing parameters are appropriate and have good dynamic performance. Besides, the battery cycles can be reduced to some extent.

This sizing method is easy to realize and can be extended to other applications, including different types of energy storage technologies. For example, in dry and sunny areas, the appropriate time constant of LPFs may be different due to the decreasing fluctuating power. Then the capacity of the supercapacitor can be determined to improve the self-consumption by considering the greatest utilization of the supercapacitor. Therefore, this method has a good prospect of engineering application.

References

[1] Tran Q., Cong Pham M., Parent L., Sousa K.: Integration of PV systems into grid: from impact analysis to solutions, 2018 IEEE International Conference on Environment and Electrical Engineering and 2018 IEEE Industrial and Commercial Power Systems Europe (EEEIC / I&CPS Europe), 2018, pp. 1-6.

[2] Weniger J., Tjaden T., Quaschning V.: Sizing of residential PV battery systems, Energy Procedia 2014, Vol. 46, pp. 78-87.

[3] Torkashvand M., Khodadadi A., Sanjareh M. B., Nazary M. H.: A life cycle-cost analysis of Li-ion and lead-acid BESSs and their actively hybridized ESSs with supercapacitors for islanded microgrid applications, IEEE Access 2020, Vol. 8, pp. 153215-153225.

[4] Wee K. W., Choi S. S., Vilathgamuwa D. M.: Design of a least-cost battery-supercapacitor energy storage system for realizing dispatchable wind power, IEEE Transactions on Sustainable Energy 2013, Vol. 4, no. 3, pp. 786-796.

[5] Javidsharifi M., Pourroshanfekr H., Kerekes T.: Optimum sizing of photovoltaic and energy storage systems for powering green base stations in cellular networks, Energies 2021, Vol. 14, no.7, pp. 1895.

[6] Gee A., Robinson F., Dunn R.: Analysis of battery lifetime extension in a small-scale wind-energy system using supercapacitors, IEEE Transactions on Energy Conversion 2013, Vol. 28, no. 1, pp. 24-33.

[7] Dulout J., Jammes B., Alonso C., A. Luna A., Guerrero J. M.: Optimal sizing of a lithium battery energy storage system for grid-connected photovoltaic systems, 2017 IEEE Second International Conference on DC Microgrids (ICDCM), 2017, pp. 582-587.

[8] Alramlawi, M. Li P.: Design optimization of a residential PV-battery microgrid with a detailed battery lifetime estimation model, IEEE Transactions on Industry Applications 2020, Vol. 56, no. 2, pp. 2020-2030.

[9] Roy P., Karayaka H., Yan Y., Alqudah Y.: Size optimization of battery-supercapacitor hybrid energy storage system for 1MW grid connected PV array, 2017 North American Power Symposium (NAPS), 2017, pp. 1-6.

[10] Ferreira K. Santos W. M., César Rueda Medina A.: Sizing of supercapacitor and BESS for peak shaving applications, 2019 IEEE 15th Brazilian Power Electronics Conference and 5th IEEE Southern Power Electronics Conference (COBEP/SPEC), 2019, pp. 1-6.

[11] Mandal S., Mandal K. K., De M., Das, G.: A new improved algorithm for optimal sizing of battery-supercapacitor based hybrid energy storage systems, 2018 Emerging Trends in Electronic Devices and Computational Techniques (EDCT), 2018, pp. 1-6.

[12] Jing W., Lai C. H., Wong S.: Battery-supercapacitor hybrid energy storage system in standalone DC microgrids: a review, IET Renewable Power Generation 2017, Vol. 11, no.4, pp. 461-469.

[13] Nichinte A. S., Vyawahare, V. A., Magare D. B.: Estimation and comparison of module temperature model coefficient for different PV technology module, 2020 3rd International Conference on Communication System, Computing and IT Applications (CSCITA), 2020, pp. 13-17.

[14] Rosewater D. M., Copp D. A., Nguyen T. A., Byrne R. H., Santoso S.: Battery energy storage models for optimal control, IEEE Access 2019, Vol. 7, pp. 178357-178391.